NUCLEAR DATA AND MEASUREMENTS SERIES

ANL/NDM-111

Fifty Years of Nuclear Fission

by

J.E. Lynn

June 1989

ARGONNE NATIONAL LABORATORY,
ARGONNE, ILLINOIS 60439, U.S.A.

NUCLEAR DATA AND MEASUREMENTS SERIES

ANL/NDM–111

FIFTY YEARS OF NUCLEAR FISSION

by

J. E. Lynn

June 1989

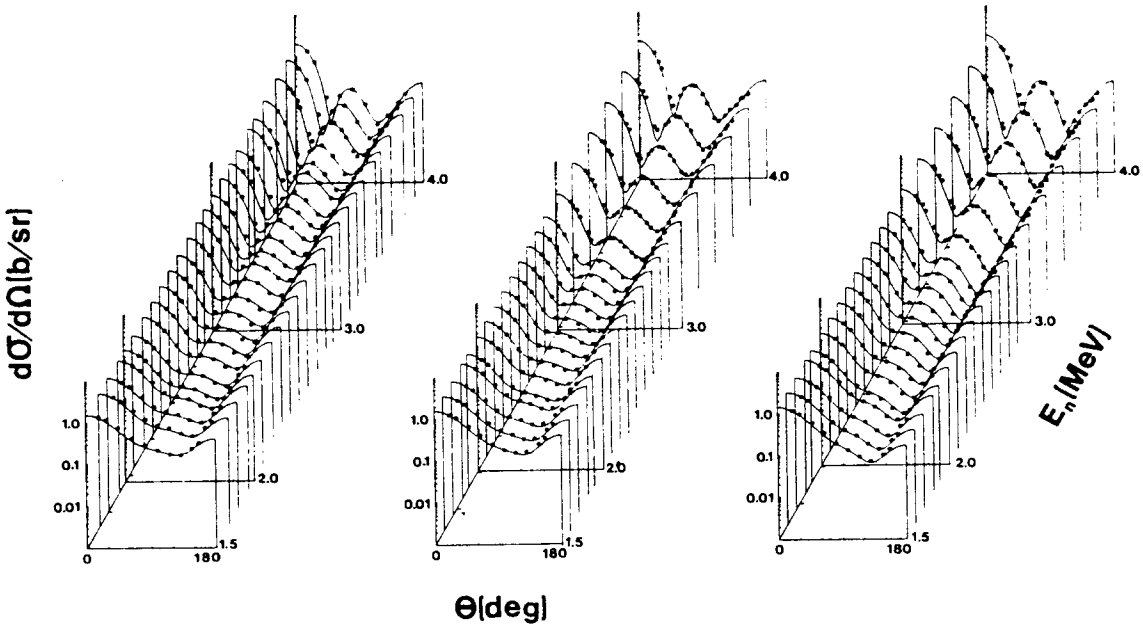

ARGONNE NATIONAL LABORATORY, ARGONNE, ILLINOIS

Operated by THE UNIVERSITY OF CHICAGO

for the U. S. DEPARTMENT OF ENERGY

under Contract W-31-109-Eng-38

ANL/NDM–111

FIFTY YEARS OF NUCLEAR FISSION

by

J. E. Lynn*+

June 1989

FISSION. Historical development and contemporary status of nuclear fission.

Engineering Physics Division
ARGONNE NATIONAL LABORATORY
Argonne, Illinois 60439
U. S. A.

---

* Work supported by the U.S. Department of Energy, Energy Reseaerch Programs under Contract W–31–109–Eng–38.

+ Argonne Fellow. Permanent address: AERE Harwell, United Kingdom.

NUCLEAR DATA AND MEASUREMENTS SERIES

The Nuclear Data and Measurements Series presents results of studies in the field of microscopic nuclear data. The primary objective is the dissemination of information in the comprehensive form required for nuclear technology applications. This Series is devoted to: a) measured microscopic nuclear parameters, b) experimental techniques and facilities employed in measurements, c) the analysis, correlation and interpretation of nuclear data, and d) the evaluation of nuclear data. Contributions to this Series are reviewed to assure technical competence and, unless otherwise stated, the contents can be formally referenced. This Series does not supplant formal journal publication but it does provide the more extensive information required for technological applications (e.g., tabulated numerical data) in a timely manner.

Additional copies [microfiche ($3.00) or xerographic (cost based on number of pages)] can be obtained by contacting:

NTIS Energy Distribution Center
P.O. Box 1300
Oak Ridge, TN 37831
U.S.A.
Comm. Phone: (615) 576–1301
FTS: 626–1301

INFORMATION ABOUT OTHER ISSUES IN THE ANL/NDM SERIES

A list of titles and authors for reports ANL/NDM–1 through ANL/NDM–50 can be obtained by referring to any report of this Series numbered ANL/NDM–51 through ANL/NDM–76, while those for ANL/NDM–51 through ANL/NDM–76 are listed in any report numbered ANL/NDM–77 through ANL/NDM–101. Requests for a complete list of titles or for copies of previous reports should be directed to:

Section Secretary
Applied Nuclear Physics Section
Engineering Physics Division
Building 316
Argonne National Laboratory
9700 South Cass Avenue
Argonne, Illinois 60439
U.S.A.

ANL/NDM–76 Alan B. Smith and Peter T. Guenther, *Scattering of Fast Neutrons from Elemental Molybdenum*, November 1982.

ANL/NDM–77 Donald L. Smith, *A Least–squares Method for Deriving Reaction Differential Cross Section Information from Measurements Performed in Diverse Neutron Fields*, November 1982.

ANL/NDM–78 A.B. Smith, P.T. Guenther and J.F. Whalen, *Fast–neutron Total and Elastic–scattering Cross Sections of Elemental Indium*, November 1982.

ANL/NDM–79 C. Budtz–Joergensen, P. Guenther, A. Smith and J. Whalen, *Few–MeV Neutrons Incident on Yttrium*, June 1983.

ANL/NDM–80 W.P. Poenitz and J.F. Whalen, *Neutron Total Cross Section Measurements in the Energy Region from 47 keV to 20 MeV*, July 1983.

ANL/NDM–81 D.L. Smith and P.T. Guenther, *Covariances for Neutron Cross Sections Calculated Using a Regional Model Based on Elemental–model Fits to Experimental Data*, November 1983.

ANL/NDM–82 D.L. Smith, *Reaction Differential Cross Sections from the Least–squares Unfolding of Ratio Data Measured in Diverse Neutrons Fields*, January 1984.

ANL/NDM–83 J.W. Meadows, *The Fission Cross Sections of Some Thorium, Uranium, Neptunium and Plutonium Isotopes Relative to* ^{235}U, October 1983.

ANL/NDM–84 W.P. Poenitz and J.W. Meadows, ^{235}U *and* ^{239}Pu *Sample–mass Determinations and Intercomparisons*, November 1983.

ANL/NDM–85 D.L. Smith, J.W. Meadows and I. Kanno, *Measurement of the $^{51}V(n,p)^{51}Ti$ Reaction Cross Section from Threshold to 9.3 MeV*, June 1984.

ANL/NDM–86 I. Kanno, J.W. Meadows and D.L. Smith, *Energy– differential Cross–section Measurement for the $^{51}V(n,\alpha)^{48}Sc$ Reaction*, July 1984.

ANL/NDM–87 D.L. Smith, J.W. Meadows, M.M. Bretscher and S.A. Cox, *Cross–section Measurement for the $^{7}Li(n,n't)^{4}He$ Reaction at 14.74 MeV*, September 1984.

ANL/NDM–88 A.B. Smith, D.L. Smith and R.J. Howerton, *An Evaluated Nuclear Data File for Niobium*, March 1985.

ANL/NDM–89 Bernard P. Evain, Donald L. Smith and Paul Lucchese, *Compilation and Evaluation of 14–MeV Neutron–activation Cross Sections for Nuclear Technology Applications: Set I*, April 1985.

ANL/NDM–90 D.L. Smith, J.W. Meadows and P.T. Guenther, *Fast–neutron–spectrum Measurements for the Thick–target $^{9}Be(d,n)^{10}B$ Reaction at $E_d = 7$ MeV*, April 1985.

ANL/NDM–91 A.B. Smith, P.T. Guenther and R.D. Lawson, *On the Energy Dependence of the Optical Model of Neutron Scattering from Niobium*, May 1985.

ANL/NDM–92 Donald L. Smith, *Nuclear Data Uncertainties (Vol.–I): Basic Concepts of Probability*, December 1988.

ANL/NDM–93 D.L. Smith, J.W. Meadows and M.M. Bretscher, *Integral Cross–section Measurements for $^{7}Li(n,n't)^{4}He$, $^{27}Al(n,p)^{27}Mg$, $^{27}Al(n,\alpha)^{24}Na$, $^{58}Ni(n,p)^{58}Co$ and $^{60}Ni(n,p)^{60}Co$ Relative to ^{238}U Neutron Fission in the Thick–target $^{9}Be(d,n)^{10}B$ Spectrum at $E_d = 7$ MeV*, October 1985.

ANL/NDM–94 A.B. Smith, D.L. Smith, P. Rousset, R.D. Lawson and R.J. Howerton, *Evaluated Neutronic Data File for Yttrium*, January 1986.

ANL/NDM–95 Donald L. Smith and James W. Meadows, *A Facility for High–intensity Neutron Irradiations Using Thick–target Sources at the Argonne Fast–neutron Generator*, May 1986.

ANL/NDM–96 M. Sugimoto, A.B. Smith and P.T. Guenther, *Ratio of the Prompt–fission–neutron Spectrum of Plutonium–239 to that of Uranium–235*, September 1986.

ANL/NDM–97 J.W. Meadows, *The Fission Cross Sections of ^{230}Th, ^{232}Th, ^{233}U, ^{234}U, ^{236}U, ^{238}U, ^{237}Np, ^{239}Pu and ^{242}Pu Relative ^{235}U at 14.74 MeV Neutron Energy*, December 1986.

ANL/NDM–98 J.W. Meadows, *The Fission Cross Section Ratios and Error Analysis for Ten Thorium, Uranium, Neptunium and Plutonium Isotopes at 14.74–MeV Neutron Energy*, March 1987.

ANL/NDM–99 Donald L. Smith, *Some Comments on the Effects of Long–range Correlations in Covariance Matrices for Nuclear Data*, March 1987.

ANL/NDM–100 A.B. Smith, P.T. Guenther and R.D. Lawson, *The Energy Dependence of the Optical–model Potential for Fast–neutron Scattering from Bismuth*, May 1987.

ANL/NDM–101 A.B. Smith, P.T. Guenther, J.F. Whalen and R.D. Lawson, *Cobalt: Fast Neutrons and Physical Models*, July 1987.

ANL/NDM–102 D. L Smith, *Investigation of the Influence of the Neutron Spectrum in Determinations of Integral Neutron Cross–Section Ratios*, November 1987.

ANL/NDM–103 A.B. Smith, P.T. Guenther and B. Micklich, *Spectrum of Neutrons Emitted From a Thick Beryllium Target Bombarded With 7 MeV Deuterons*, January 1988.

ANL/NDM–104 L.P. Geraldo and D.L. Smith, *Some Thoughts on Positive Definiteness in the Consideration of Nuclear Data Covariance Matrices*, January 1988.

ANL/NDM–105 A.B. Smith, D.L. Smith, P.T. Guenther, J.W. Meadows, R.D. Lawson, R.J. Howerton, and T. Djemil, *Neutronic Evaluated Nuclear–Data File for Vanadium*, May 1988.

ANL/NDM–106 A.B. Smith, P.T. Guenther, and R.D. Lawson, *Fast–Neutron Elastic Scattering from Elemental Vanadium*, March 1988.

ANL/NDM–107 P. Guenther, R. Lawson, J. Meadows, M. Sugimoto, A. Smith, D. Smith, and R. Howerton, *An Evaluated Neutronic Data File for Elemental Cobalt*, August 1988.

ANL/NDM–108 M. Sugimoto, P.T. Guenther, J.E. Lynn, A.B. Smith, and J.F. Whalen, *Some Comments on the Interaction of Fast–Neutrons with Beryllium*, November 1988.

ANL/NDM–109 (Not yet in print.)

ANL/NDM–110 D.L. Smith and L.P. Geraldo, *A Vector Model for Error Propagation*, March 1989.

TABLE OF CONTENTS

FIFTY YEARS OF NUCLEAR FISSION

by

J. E. Lynn*

Engineering Physics Division
Argonne National Laboratory
Argonne, Illinois 60439
U. S. A.

ABSTRACT

This report is the written version of a colloquium first presented at Argonne National Laboratory in January 1989. The paper begins with an historical preamble about the events leading to the discovery of nuclear fission. This leads naturally to an account of early results and understanding of the fission phenomena. Some of the key concepts in the development of fission theory are then discussed. The main theme of this discussion is the topography of the fission barrier, in which the interplay of the liquid–drop model and nucleon shell effects lead to a wide range of fascinating phenomena encompassing metastable isomers, intermediate–structure effects in fission cross–sections, and large changes in fission product properties. It is shown how study of these changing effects and theoretical calculations of the potential energy of the deformed nucleus have led to a broad qualitative understanding of the nature of the fission process.

---

* Argonne Fellow. Permanent address: AERE Harwell, United Kingdom.

Fifty Years of Nuclear Fission

J E Lynn

Argonne National Laboratory, Illinois 60439

1. Introduction

The first papers announcing the discovery of neutron-induced fission of the nucleus of the uranium atom were published in January and February of 1939, almost exactly 50 years ago. Therefore I feel honoured to have been invited to present a colloquium on fission at this particular time and at this particular Laboratory, for the roots of Argonne are especially strongly entwined with the early events in fission; the research based on the World's first self-sustaining nuclear fission chain reaction, Fermi's famous graphite pile, built under the stand of the University of Chicago football field, was soon moved out into the Argonne forest to be later developed into the Argonne National Laboratory.

I must confess that I did not fully realise the magnitude of what I had undertaken in suggesting the title of this talk until the printed notice arrived in my office. Fifty years is a long time, and because of the awesome applications of fission as well as the richness and fascination of the phenomenon itself, a vast amount of research has been done and a vast literature exists on the subject. In my talk today I shall not touch upon fission technology at all. What I shall present here is a broad survey of the development of our understanding of the phenomenon from its discovery until the present day. Because of limitations of space I shall also confine my presentation to the "classical" study of fission, i.e., spontaneous fission and fission at relatively low excitation energies induced by light particles or photons. Fortunately there is an underlying relatively simple theme in this story, which can be called "the topography of the fission barrier".

The outline of this talk is as follows. In Section 2 I give a historical preamble. This fairly naturally leads into a discussion of the early understanding and early experimental knowledge of the fission phenomenon in Section 3. Early work using statistical models to describe some of the most puzzling features of fission is touched upon in Section 4. Section 5 contains some account of the understanding achieved by the introduction of concepts of quantised collective motion into fission theory. These three sections largely cover the development of the subject in its first quarter century. The second quarter century is largely dominated by the penetration of shell model concepts into fission theory. Section 6 describes the confluence of the important theoretical development and dramatic experimental discoveries that brought the

realisation of the vital role that shell effects play. These at first concerned the overall decay rate of nuclei by fission, but later their role in forming the properties of the ultimate fission products was discovered; this is described in Section 7.

2. Historical preamble

Artificial radioactivity was discovered by Irene Curie and F.Joliot in 1934. The employed projectiles were alpha-particles. Fermi had the idea of using neutrons, discovered two years earlier, to find new radioactive nuclides; these had the advantage of not having to overcome a Coulomb barrier to penetrate the nucleus, and, after the discovery of the great moderating power of hydrogeneous materials, were found to be extremely effective in inducing artificial radioactivity. The unstable nuclides discovered in this way from 1934 onwards were predominantly beta-active, the nuclear reaction being the formation of a compound nucleus (Z,A+1) by addition of a neutron to the target nucleus (Z,A); radiative de-excitation of the compound nucleus is followed by beta-decay to give the nucleus (Z+1,A+1), which is closer to the valley of stability.

This general mechanism, which was well established by the methods of nuclear chemistry, was assumed as the guiding hypothesis when Fermi and his group came to interpreting the results of bombarding uranium with neutrons. Thus, after establishing chemically that some of the principal activities observed did not behave like any of the elements between lead and uranium, Fermi concluded that they belonged to new elements beyond uranium[1]. Some participants of that era, notably Segre[2], then one of Fermi's principal collaborators, have noted that the German chemist Ida Noddack pointed out[3] that the Rome group had not proved the "new" elements did not behave chemically like much lower mass elements, thus not precluding the break-up of the uranium nucleus into massive fragments. Later as these neutron reactions were explored much more fully by Hahn, Meitner and Strassmann and then by Hahn and Strassmann alone after Meitner left Germany, they were found to be very complex in the range of decay half-lives and the chemical behaviour they showed. Chains of beta-decays were hypothesized, ending in multiple isomers of elements called variously eka-gold, eka-platinum etc. with chemical properties often similar to those of radium and neighbouring elements. But Curie and Savitch, working in Paris, showed that one of the products of neutron bombardment was extremely similar, chemically, to lanthanum[4]. In response to this and, after devising very methodical tests it was finally proved by Hahn and Strassmann that some of the new reaction products were chemically identical with such elements as barium and lanthanum, and they were forced to the conclusion that they were indeed isotopes of these much lighter elements[5].

The pre-publication copy of the paper announcing these startling results was sent to Lise Meitner in Sweden shortly before Christmas 1938, and at that time she was joined by Otto Frisch, her nephew, where together they puzzled over their interpretation. They soon realized that the phenomenon was explicable within the dominating concept of nuclear theory at that time, the liquid drop model. The nucleus, behaving as an electrically charged liquid drop, after a certain amount of initial elongation against resistance by the surface tension, could split, under the influence of electric repulsion, into two comparable sized parts. Their initial calculations supported this interpretation, and they also realised that the Weizsäcker semi-empirical formula for nuclear masses, a formula of which the chief ingredients were terms analogous to the volume, surface and

coulomb energies characteristic of a liquid drop, indicated that such a splitting reaction was strongly exothermic with an energy release of approximately 200 MeV.

Frisch named the phenomenon "fission" from the term for biological cell division. On his return to Copenhagen he was able to inform Neils Bohr of the new ideas just as the latter was about to set sail for the USA. Hahn and Strassmann's paper was published in Naturwissenschaften[5] early in 1939. At about the same time Meitner and Frisch's interpretation was published in Nature[6], along with a paper by Frisch reporting an ionization chamber measurement of the very great energy released in the reaction[7].

At this point it is of some interest to digress and return to the matter of the 1935 paper by Ida Noddack[3], in which she showed that Fermi's group had not eliminated the possibility of middle range elements being formed in the neutron reaction with uranium. In an interesting paper published in Nuclear Physics last year[8] Pieter van Assche shows how close Ida Noddack was to the observation of uranium fission. Van Assche establishes that she with her (later) husband Walter Noddack and Otto Berg in Berlin almost certainly observed uranium fission products as early as 1925. This team was searching for the missing element Z=43 in a range of ores. In a number of ores with substantial uranium content, but no others, they found very weak X-ray lines with the right energies to be the K lines of Z=43, which they named masurium. Van Assche argues that the intensity of these lines is consistent with the occurence of the element as a fission product from spontaneous fission of uranium. In that era the team's announcement of the discovery of Z=43 was discredited, and later (1937) Perrier and Segre artificially created and observed it as technetium. If the earlier discovery had been accepted (and with it the association of the element with uranium) Ida Noddack's paper may well have influenced Fermi towards a much earlier discovery of uranium fission. One can only speculate on the effect of this on World history.

3. Early results in fission

When Niels Bohr brought the news of nuclear fission to the USA experimental work on the new phenomenon immediately started there, and also in France following the publication of Hahn and Strassmann's paper. The publication of new results was very patchy, largely owing to the efforts of Leo Szilard who was extremely concerned about the weapons potential of the nucleus and wished scientists to submit to voluntary censorship in the dangerous political atmosphere of the time[9]. But the main features of uranium fission were quickly established. The extremely high energy release observed by Frisch was confirmed by Dunning and his group at Columbia[10]; the release of neutrons in the fission event was soon established by Anderson,Fermi and Halstein[11], by Halban, Joliot and Kowarski[12], and by Szilard and Zinn[13], giving a measure of the internal excitation energy of the fission products; neutron fission cross-sections were measured[10,13,14]; delayed neutrons were discovered[15]; and a crude picture of the fission product mass-yield curve was built up[16]. It was found that intermediate (resonance) fission of uranium was not measurable, in spite of the fact that a large resonance was known to exist in the uranium radiative capture cross-section at an energy then believd to be about 25 eV. But it was known that fission could be induced in uranium and thorium by fast neutrons (energy about 2 MeV).

In the first few months of 1939 Bohr and Wheeler laid down the foundations

of the liquid drop theory of fission[17]. They established the concept of the fissility parameter, explaining how the charge and mass numbers in the ratio Z^2/A measured the closeness of the nucleus to critical instability against fission. The nature of the potential barrier against fission - a col or saddle-point in the liquid drop deformation energy surface in the space of the nuclear deformation parameters (see Fig.1) - was explored, and the rate for the system to cross that barrier was deduced from the theory of chemical reaction rates. From this and Bohr's earlier theory of the compound nucleus the essential elements of the theory of fission cross-sections could be built.It was also deduced that the thermal-neutron induced fission of uranium could only take place through the 0.7% abundant ^{235}U nucleus[18]. The difference in behaviour between this and the main isotope ^{238}U could be explained by the greater neutron separation energy of the compound nucleus ^{236}U for the former case bringing its excitation energy close to or above the fission barrier. These results were published in their classic paper in Physical Review in September, 1939. Not long afterwards, the U.S. physicists submitted themselves to voluntary censorship as events plunged towards World War.

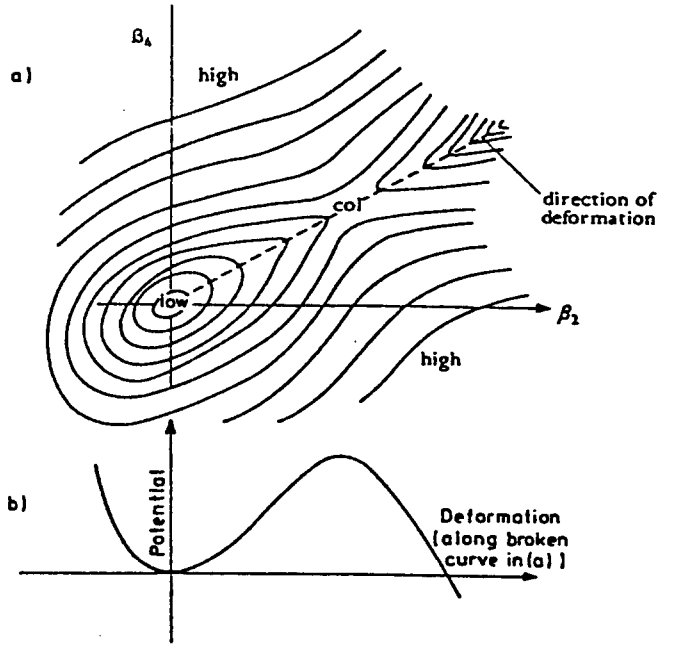

Figure 1.Schematic diagram of potential energy contours as function of quadrupole and hexadecapole deformation parameters of liquid drop. Lower part shows the minimum energy trajectory for increasing elongation.

4. Statistical models

For the next quarter century the liquid drop model remained the dominant theory of nuclear fission, receiving much refinement in the hands of Swiatecki and his collaborators, Hill and Wheeler, Frankel and Metropolis and others, while the experimental data, especially on nuclides other than those of uranium expanded apace. The liquid drop model persisted in spite of the fact that in nuclear structure and reaction theory the liquid drop concept was all but discarded by the advent of the shell model in 1949 and the optical model in 1954. Its persistence was also in spite of the fact that the model found major difficulties in explaining some of the major phenomena exhibited in fission by the nuclides in the actinide group of elements.

One particularly severe problem was the mass dependence of the yield of individual fission products. In the liquid drop model the division of the nucleus was expected to be symmetric, implying a mass-yield curve that peaks at half the mass of the fissioning nucleus. The width of the peak depends on the detailed nature of the potential surface near and beyond the saddle-point and on the inertial tensor for the dynamical motion within this potential landscape. Such mass yield behaviour is in fact found for fission of much lighter nuclides than uranium, and also for uranium itself at very high excitation energies. But at low excitation energies of the actinides the mass yield is highly asymmetric;

the heavy fission product is peaked about mass 140, while the light product is centred about the complementary mass, which is about 90 for the light actinides and increases to about 110 for Cf.

The basic assumption of the statistical model is that all energetically accessible elements of phase space are equally likely final states of the system. This principle is already embodied in Bohr and Wheeler's expression for the transition rate across the barrier[17]. This can be expressed as a transmission coefficient for the system crossing the barrier, and is given by

$$T_f = 2\pi\Gamma_f/D = N = \int_{E_f}^{E} dE' \ \rho^*(E'-E_f)$$

where N is the number of levels of 'intrinsic' excitation available to the nucleus in the transition state as it crosses over the barrier (Fig.2); it is here expressed in terms of the level density ρ^* at the saddle point, where the available excitation energy is $E - E_f$, E_f being the potential, or activation, energy at the saddle.

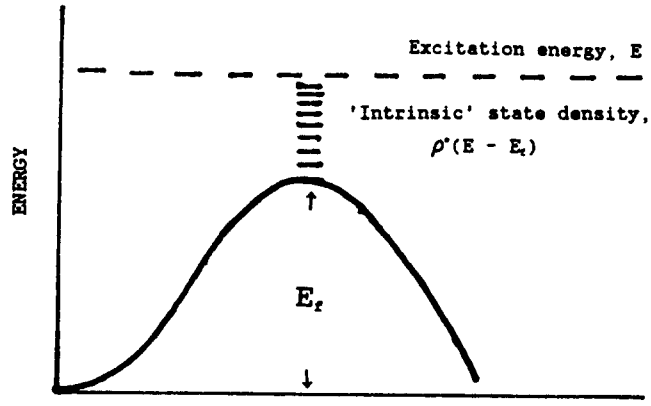

Figure 2. Intrinsic states available at saddle point.

Fong[19] employed the same principle in attempting to explain the mass-yield curve. He assumed in this that the final states of the system were those of the nascent fragments at the point of rupture, the scission point. The total energy available for any fission product pair can be calculated from the Weizsäcker mass formula, to which is added the excitation energy of the original compound nucleus. At the scission point, part of this energy is locked up as mutual Coulomb repulsion energy of the nascent fragments and their deformation energy. There will also be some relative energy of motion of the fragments. The remainder is available for intrinsic excitation of the fragments, and the number of combinations (within each pair) of intrinsic states thus accessible is proportional to the yield of the pair. But in calculating the energy available for intrinsic excitation Fong allows for the extra stability of fragments near shell closures. This gives extra energy and hence increased yield probability for "magic" fragments such as ^{132}Sn. Such an approach accounted, at least qualitatively, for the asymmetric mass yield curve, which peaks for the actinides at about A = 140. The approach can be criticized in detail, however, on at least two counts: shell effects on the level density (which will decrease the number of intrinsic states available and hence tend to cancel the effect of increased fragment stability) are smoothed out; and until the much later work of Strutinsky there was no sound way of calculating the deformation energy of the nascent fragments.

5. Quantised collective motion and the channel theory

Some of the other striking experimental information on fission collected by the early 1950s included strong angular dependences of the fission product

emission, especially near the fission barrier energy, and strong fluctuations of the fission widths of the resonances in slow neutron cross-sections. Both of these features were unexpected within the theory at the stage to which it had then developed. They were resolved by Aage Bohr[20] who introduced the concept of saddle point channels in 1954.

The expression governing the rate of fission, eq.1, was generalised for a model of quantum barrier tunnelling by Hill and Wheeler[21] in 1953. On the assumption of an idealised barrier of inverted harmonic oscillator form the transmission coefficient becomes

$$T_f = 2\pi\Gamma_f/D = N_{eff} = \int_{E_f}^{\infty} dE' \rho^*(E'-E_f) \{1+\exp[2\pi(E'-E)/\hbar\omega]\}^{-1} \quad (2)$$

where N_{eff} is the effective number of energetically available states of "intrinsic" excitation available at the saddle point. For relatively low excitation energies a continuous level density function is not a good representation of the level scheme in nuclear studies, and the same may apply for low excitation energy at the saddle point. Aage Bohr therefore replaced the integral in eq.2 by a sum over quasi-discrete states of intrinsic excitation:

$$T_f = \sum_i \{1+\exp[2\pi(E_i-E)/\hbar\omega]\}^{-1}$$

Furthermore, he considered the possibility that these states retain some quantal properties analogous to those found in normal nuclear level structure. For an actinide nucleus with the strong elongation it would possess at the saddle point such properties would typically be those collective rotational and vibrational characteristics postulated and studied by Bohr and Mottelson over the previous few years. For example, an even compound nucleus could be expected to have a lowest intrinsic state at the saddle point with zero spin and even parity and, if the fissioning nucleus still possessed axial symmetry, a spin projection on the major axis of $K = 0$. Built on this state one could expect a rotational band limited to the spin and parity sequence $I^\pi = 0^+, 2^+, 4^+, \ldots$. At higher energies one could expect a vibration of reflection, or mass, asymmetry character with $K^\pi = 0^-$, $I = 1,3,5,\ldots$, and a gamma-vibration about axial symmetry with $K^\pi = 2^+$, $I = 2,3,4,\ldots$, and so on. The energies of these rotational bands,

$$E_i = E_I - E_R + (\hbar^2/2\Im)[I(I+1) - K(K+1)]$$

are governed by a moment of inertia $\Im$ that can be expected to be considerably larger than that for the nucleus in its normal ground state deformation. The transition state for a compound nucleus of definite total angular momentum and parity will be a superposition of intrinsic states of the same spin and parity, but with K-values and wave-functions of the kinds illustrated above; their amplitudes within the transition state will be governed by a tunnelling factor related to the Hill-Wheeler form.

In a nuclear reaction the total spin projection on a well-defined laboratory axis, such as the projectile beam direction, can be limited to a very narrow range of values, e.g. $M = \pm 1$ for electric dipole photon absorption (giving $I = 1$ for an even target), or $M = \pm\frac{1}{2}$ for neutrons on an even target (giving $I = \ell \pm \frac{1}{2}$, where ℓ is the neutron orbital angular momentum). Hence, if only one or a few intrinsic states of the above type have high amplitude in the transition

state, there is strong control of the direction of the major symmetry axis of the fissioning system in relation to the laboratory axis (see Fig.3), giving rise to strong angular distributions of the fission products (Fig.4). These are typically sideways emission for electric dipole photofission, or forward and backward peaked emission for fast-neutron induced fission of an even target with $K = \frac{1}{2}$.

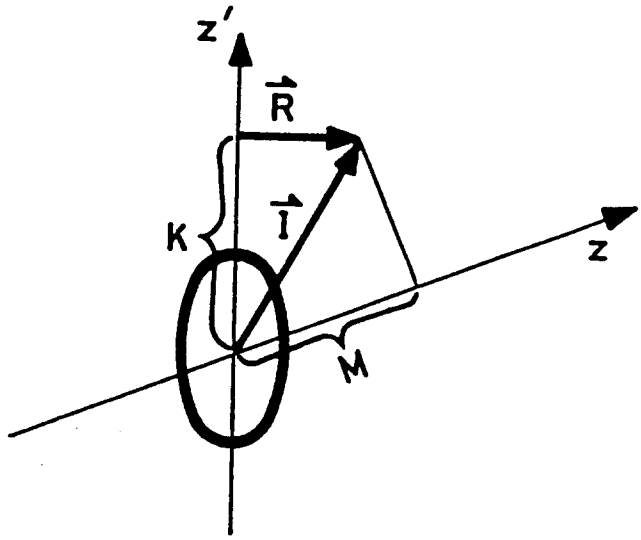

Figure 3. Angular relationships for a spheroidal nucleus with total spin I, rotation R, and spin projections M and K on laboratory and symmetry axis, respectively.

Another example of the influence of intrinsic states of such specific character comes from the properties of the slow neutron resonances in fission cross-sections. Slow neutron resonances characteristically show strong fluctuations in their peak magnitudes and widths from one resonance to another. In the non-fissile case these fluctuations can normally be attributed to the partial width for neutron absorption. The fluctuations found in this quantity are those to be expected for a partial width of a single channel process. The total radiation width, which is normally the other important quantity governing the decay of the resonance state, is, on the other hand, a sum over a large number of partial widths of independent radiative decay channels. In consequence it is found to be virtually constant from resonance to resonance. By analogy, it would be expected that the fission width, which leads also to a large number of channels for many different pairs of fission products in a large number of different states of excitation, would also be constant. Experimentally this is found not to be so; fission widths fluctuate almost as widely as do neutron widths. The reason is that they are not independent; a large spectrum of fission product states stems from a single intrinsic component in the transition state, and it is this intrinsic component that is to be regarded as the channel. The wide fluctuation of the fission widths shows that only a few intrinsic states are effective in low energy fission.

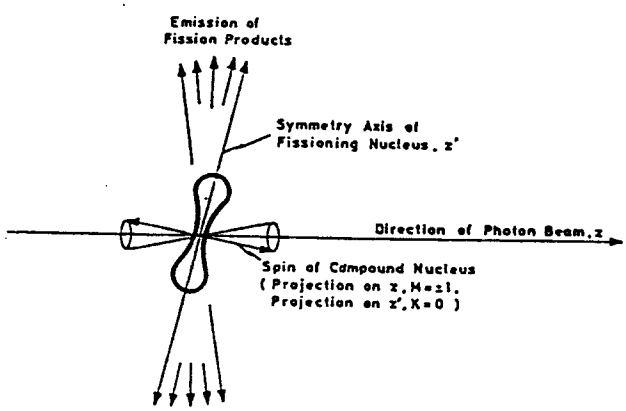

Figure 4. How spin relationships of cold nucleus at the saddle point explain fission product angular distribution from electric dipole photofission.

Another demonstration of the significance of the intrinsic states (which we shall henceforth call fission channels) is to be found in the neutron fission cross-section of ^{239}Pu. The levels corresponding to the s-wave resonances of this cross-section have spin-parity 0^+, 1^+. The 0^+ resonances have fission widths averaging a few eV, while the 1^+ fission widths average about 100 meV. The

difference can be attributed to the large energy difference expected for the channels in the two cases (equal at least to the pairing gap).

6. Shape isomers and cross-section intermediate structure

The major significance of shell effects in the fission process was realised about 1967 as a result of the confluence of some striking experimental discoveries and new theoretical developments. On the experimental side the first discovery was the occurence of spontaneously fissioning isomers[22]; the fission half-lives of these are shorter than ground state spontaneous half-lives by up to twenty orders of magnitude, indicating an excitation energy of about 3 MeV or more. At such a high energy it becomes extremely difficult to explain the inhibition of gamma-decay by any normal process. At about the same time new theoretical developments by Strutinsky[23], which considered shell effects for nuclei of extended deformation, led to a novel explanation of such isomerism. The interpretation was confirmed by discovery of narrow intermediate structure in fission cross-sections[24,25].

The source of shell effects in nuclear deformation energy is illustrated schematically in Fig.5. This shows the energy eigenvalues of the single particle orbitals in a spheroidal harmonic oscillator potential well (without spin-orbit coupling or coulomb interaction). As well as the expected strong clustering of energy levels at the magic particle numbers for a spherical well, similar effects are found at other deformations, especially axis ratios 2:1 and 3/2:1. Systems with particle numbers equal to or just below these new magic numbers can be expected to have special stability at such deformations.

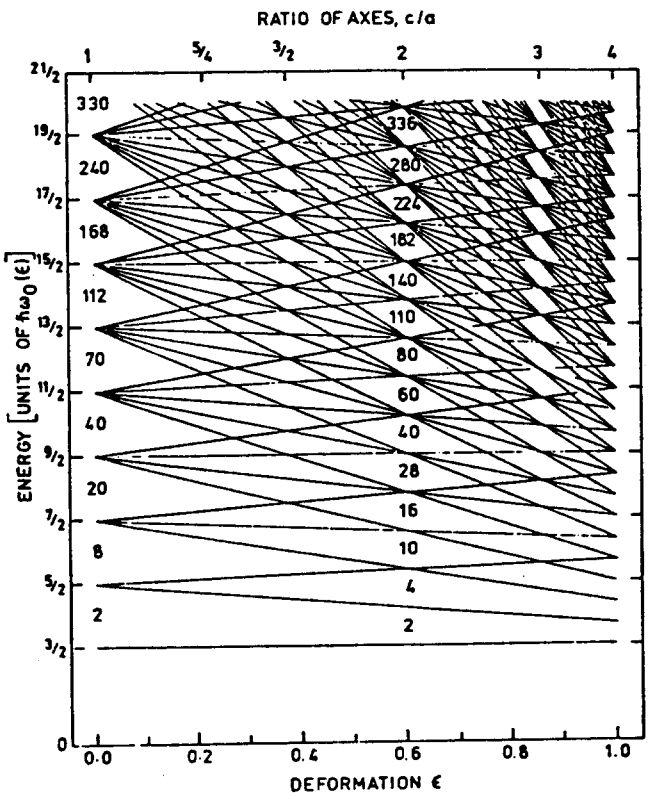

Figure 5. Eigenvalues of a spheroidal harmonic oscillator without spin-orbit coupling, showing shell gaps at axis ratios of 2:1 and 1.5:1 as well as those for sphere.

Starting with such considerations Strutinsky devised a shell correction energy (and pairing energy) which, when added to the liquid drop model energy, gave remarkable fission barrier behaviour for the actinides, such as that illustrated in Fig.6. Such a barrier provides an immediate explanation for the spontaneously fissioning isomers as metastable states isolated at the extended deformation of the secondary dip in the deformation energy curve. It is also to be noticed that the theory gives a special stability to the fission barrier of the actinides as a function of Z^2/A. The peak of the liquid drop barrier moves to lower deformations and decreases in magnitude as Z^2/A increases, while the shell correction term does not change much. In

consequence, the outer barrier is dominant for the low charge actinides, only to decline and be replaced in importance by the inner barrier as the proton number increases.

Experiments on the properties of the shape isomers were a dominant feature of fission research in the late 1960s and early 1970s. In addition to identification of the isomers by half-life, measurement of their excitation energy and yield relative to prompt fission were vital. The mechanism for population of a shape isomer is illustrated in Fig.7. By exciting a heavier nucleus the rate of population of the isomer by neutron evaporation can be observed as a function of excitation energy. Simple model excitation functions are illustrated in Fig.8. It is clear that maximum precision in determination of the threshold for formation of the isomer is achieved in principle by using a one neutron evaporation reaction, but for exploring a full range of nuclides it is necessary to use a range of charged projectiles, which, to overcome the Coulomb barrier, give rise to excitation energies in the two-, and even three-, neutron evaporation range.

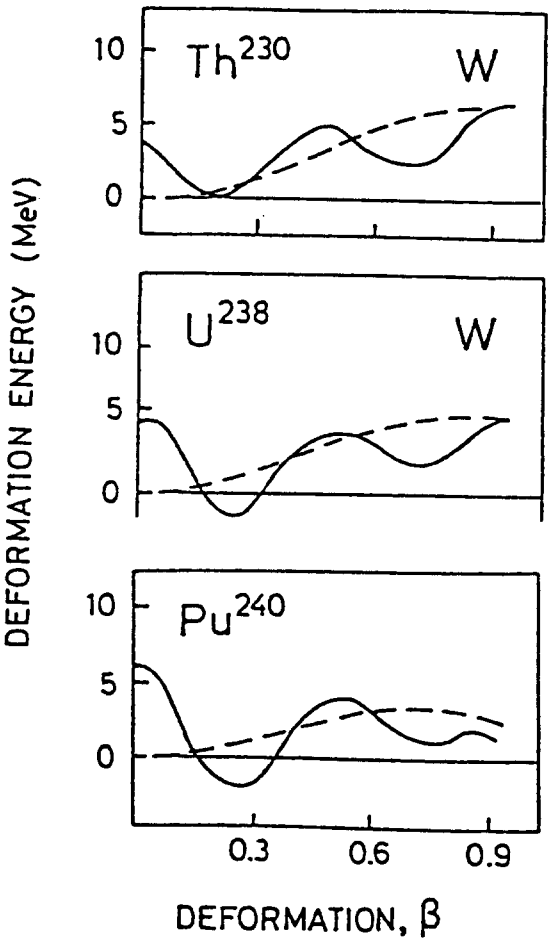

Figure 6. Typical calculated fission barriers with shell corrections. Broken curve is the liquid drop barrier.

A typical set of experimental data and a model fit are shown in Fig.9. From data such as these isomer excitation energies can be obtained with an accuracy of 0.3 MeV or so, and also, from the asymptotic ratio of delayed to prompt fission yield, some measure of the outer barrier height of the evaporating nucleus. Such data, allied with the fission half-life information, give a good picture of the comparative stability of the secondary well and the decreasing strength of the outer barrier from the plutonium isotopes through the curium isotopes. These indications are in semi-quantitative agreement with the more sophisticated calculations developed out of the Strutinsky theory by many workers in the 1970s.

For nuclides lighter than plutonium, the yield of isomer fission relative to direct fission falls markedly. This is ascribed to the greater outer barrier height and decreased inner barrier; this allows significant competition from gamma decay of the isomer, cascading through states associated with the normal deformation of the primary well down to the ground state. Such delayed gamma rays have been observed. An example is ^{238}U, in which a cascade has been observed and interpreted as that from an isomer with half-life 190 ns at 2.56 MeV excitation energy. The spontaneous fission decay has also been observed by neutron inelastic scattering (Fig.10). A simple neutron evaporation model (dashed curve of Fig.10)

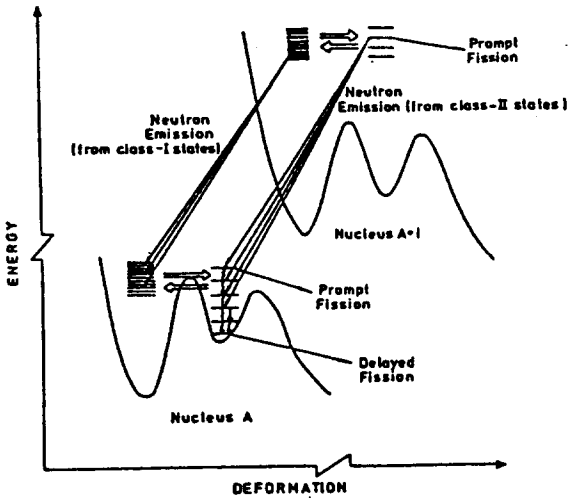

Figure 7. Population routes for formation of a shape isomer.

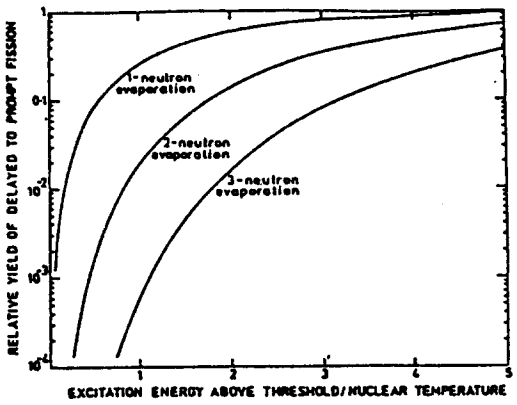

Figure 8. Isomer excitation functions in simple equi-temperature level density model.

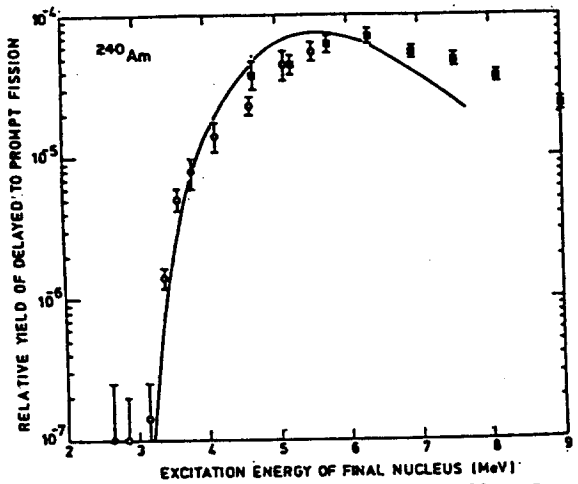

Figure 9. Excitation of the 0.9ms isomer of ^{240}Am. Data are from the (p,2n) reaction[26] and the (d,2n) reaction[27].

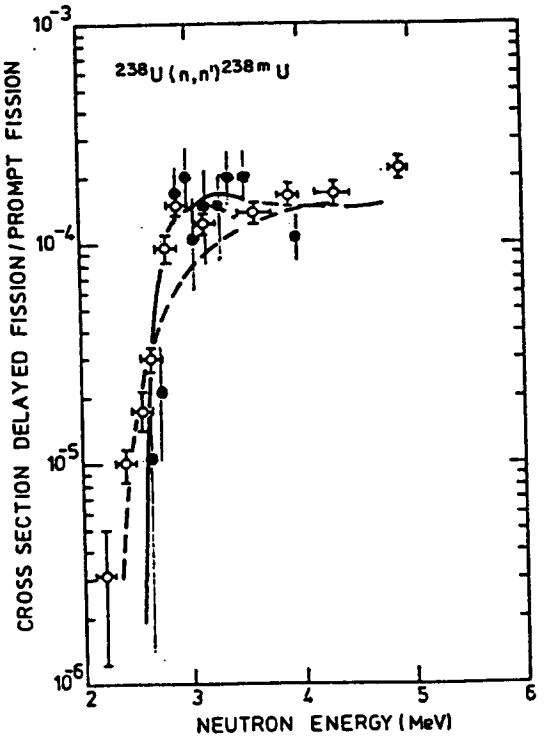

Figure 10. Excitation of shape isomer in ^{238}U by inelastic scattering.

seems to imply too low an isomer energy, but a model that takes the energy gap and vibration-rotation band structure of the ^{238}U level structure into account gives a very reasonable fit, based on the 2.56 MeV isomer hypothesis. In this case, the fission branch of the isomer is about one order of magnitude weaker than the gamma branch.

Some spectacular work has also been done on the spectrosopy of excited states of high deformation that feed the isomer. The pioneering example is illustrated in Fig.11. The conversion electron spectrum associated with the cascade through the rotational band built on the shape isomer of ^{240}Pu has been observed by Specht *et al.*[28]. The measurement of the rotational band energy

spacings indicates that the moment of inertia is about double that of the ground state band, and thus constitutes confirmation of the strongly deformed shape of the isomer.

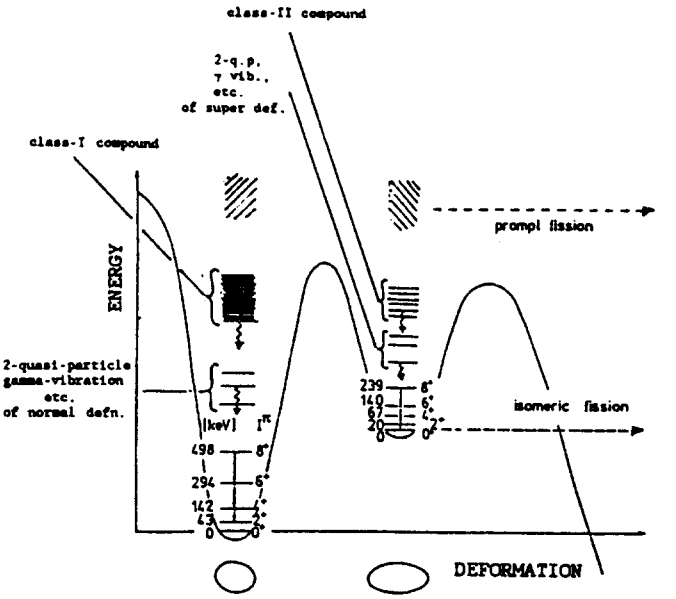

Figure 11. Rotational bands of ^{240}Pu. The band in the secondary well has been measured by Specht et al.[28] Also shows classes of states of higher excitation.

Narrow intermediate structure in fission cross-sections, first discovered by Fubini *et al.*[23] and Migneco and Theobald[24], is illustrated in Fig.12. The upper part of the figure shows the total neutron cross-section[29] of ^{240}Pu. The fluctuating strength of the many resonance peaks is a consequence of the random fluctuations in their neutron widths. The lower part of the figure shows the completely different nature of the fission component of the cross-section. Each cluster of fission resonances is interpreted as the effect of a highly deformed "class-II" compound state high in excitation energy above the shape isomer but still confined by the inner and outer barrier peaks (see Fig.11). The results of detailed examination of these intermediate resonances (e.g. Fig.13) gives insight into the nature of the modulation of the fission cross-section by the class-II state. For example, in Fig.13 the rather weak fine-structure resonance at 781 eV has much the largest fission width of the group[30] and therefore can be interpreted as being a nearly pure class-II state. Its overall strength is low because its very small neutron width is picked up only by its very weak coupling, through the inner barrier, with its dense class-I neighbours of normal deformation.

Another example is shown in Fig.14. In this, the neutron fission cross-section of ^{238}U in the region of 720 eV[31], the cross-section is two orders of magnitude lower than in the previous case, a consequence clearly of the fission

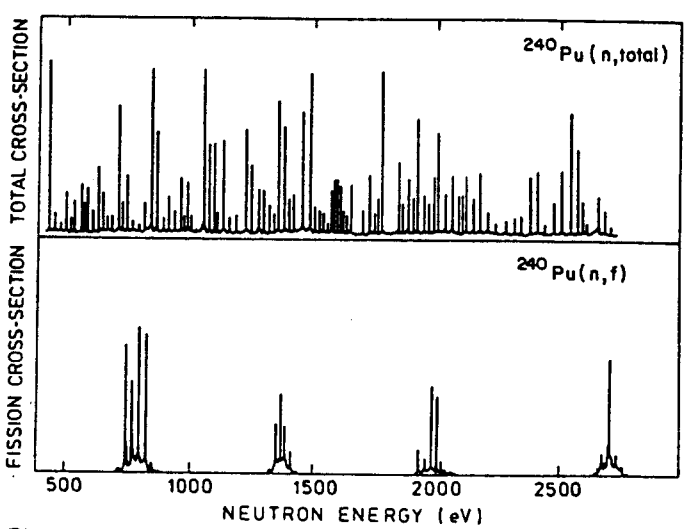

Figure 12. The neutron total and fission cross-sections of ^{240}Pu in the resonance region.

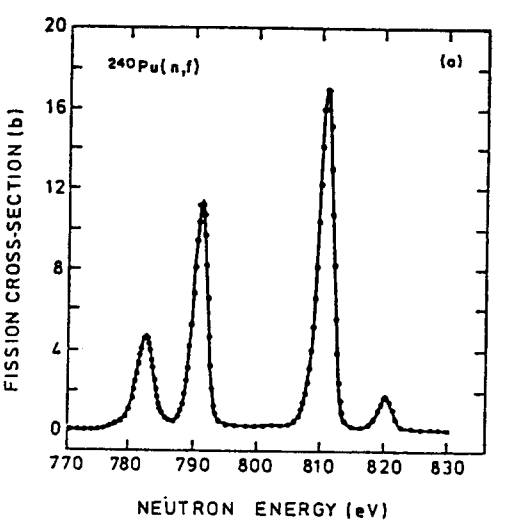

Figure 13. The neutron fission cross-sections of ^{240}Pu in the region of 800eV.

barrier (relative to zero neutron energy) being some hundreds of keV higher. The intermediate resonance spacing is about the same. The main resonance in the ^{238}U fission cross-section has been identified as a nearly pure class-II state by careful determination of its total radiation width[32], which is lower than the radiation width of the multitude of class-I resonances in the total cross-section by a factor of five. Analysis of the parameters of this and higher intermediate resonances suggests that the inner and outer barriers are both much lower than those needed to replicate the energy dependence of the fast neutron fission cross-section at 1 MeV neutron energy and above. Reconciliation of the latter with the intermediate structure parameters can be achieved by postulating that the observed fission in the resonance region is delayed fission following radiative decay of the class-II states to the shape isomer. For this explanation to be valid the isomer would have a half-life of the order of or less than the time-of-flight resolution of the resonance region measurement and a branching ratio to fission of about one fifth.

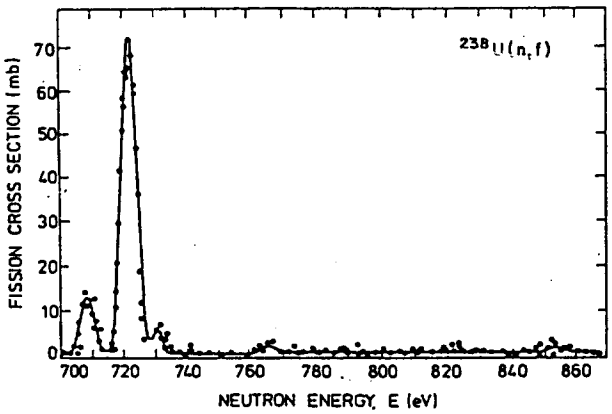

Figure 14. Intermediate structure in the neutron fission cross-section of ^{238}U.

In the cross-sections of the thorium and protoactinium nuclides another kind of resonance effect occurs. This is a giant resonance effect[33], as illustrated in Fig.15 for the neutron fission cross-section of ^{230}Th. Here the width of the resonance is on the 10 keV scale and spacing of such resonances is on the scale of several hundred keV. Explanation of this as intermediate structure modulated by class-II states of a secondary well is inconsistent with the systematics of the parameters of the double-humped barrier as calculated by theory. Careful calculations of the barriers of the light actinides indicated that the outer barrier could be split by a shallow tertiary well. If this is the case, the giant resonances observed in the thorium group of nuclides could be due to low phonon ß-vibrations (vibrations in the fission elongation mode) in the tertiary well. If the inner barrier is low, as suggested by theoretical systematics, such a simple configuration class-III state could connect directly to the class-I fine structure states, which of course are too closely spaced to be resolved in the energy region of Fig.15.

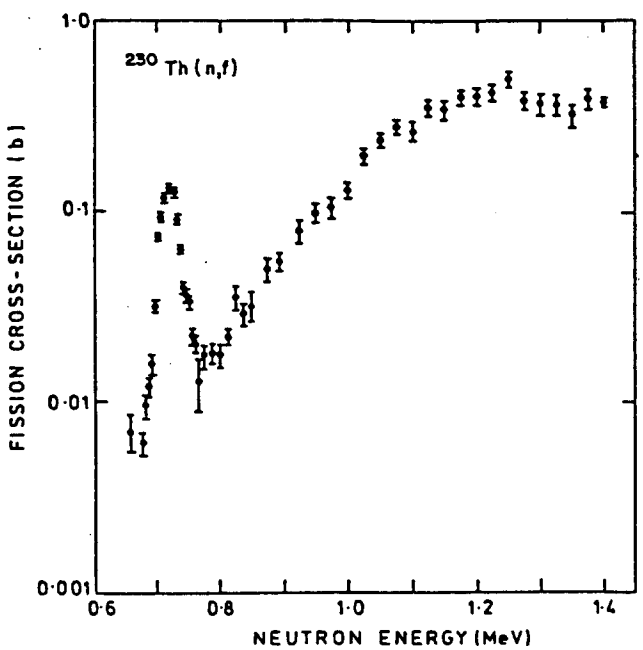

Figure 15. The neutron fission cross-section of ^{230}Th.

Detailed analysis of the kind of data shown in Fig.15 brings into play even more sophisticated features of the fission barrier topography. A contour diagram[34] of the outer fission barrier of ^{234}Th is shown in Fig.16. The deformation variables employed are elongation and degree of reflection asymmetry (across a plane perpendicular to the cylindrical symmetry axis of the elongated nucleus). This diagram illustrates that it is characteristic of the outer barrier of the actinides for the minimum energy path to be reflection asymmetric; this is lower by several MeV than the reflection symmetric route to fission. The tertiary well of the thorium nuclides is thus calculated to have reflection asymmetric, or pear-shaped, deformation.

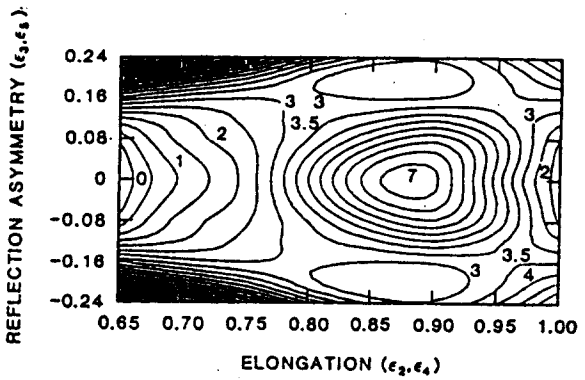

Figure 16. Potential energy calculations for the outer barrier region of a typical thorium nuclide.

The basic configuration of the class-III state of the neighbouring odd-A (compound) nucleus ^{231}Th is thus expected to be a ß-vibrational mode coupled to a single-particle neutron mode of extended Nilsson character, coupled to a rotational mode. Thus the apparently single peak of Fig.15 can be expected to contain several members of a rotational band, and some of the structure due to this has indeed been observed[35] (see Fig.17a). The reflection asymmetric character

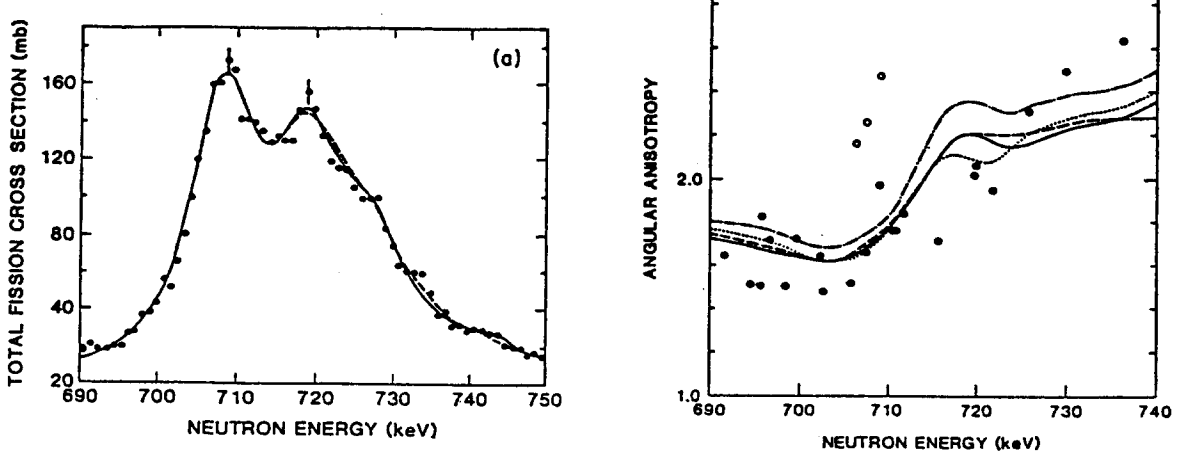

Figure 17. High resolution cross-section and fission product angular anisotropy data for ^{230}Th(n,f). The curves are fits using reflection asymmetry, Coriolis coupling and parity-dependent fission strengths.

of the tertiary well will bring down an extra, nearly degenerate, rotational band of opposite parity to that of the original Nilsson band. It is difficult, if not impossible, to fit all the data on the ^{230}Th(n,f) giant resonance without recourse to this extra band. Even more detailed fitting includes the possibility of coriolis coupling with neighbouring class-III states differing in spin projection K by one unit and the possibility of the class-III fission and coupling widths differing for the opposite parity bands. Some examples of such detailed fitting

are shown in Fig.17. The class-III state responsible for this resonance has $K^{\pi} = 1/2^{+}$; the nearly degenerate opposite parity band is separated form it by only about 17 eV; the moment of inertia constant is $\hbar^2/2\Im \approx 1.1$keV; the strength of Coriolis coupling is consistent with the existence of a known $K = 3/2$ state; and the odd-parity states have a fission (or coupling) width about one fifth of that of the even parity states[36].

7.Topography between saddle and scission; mass yield behaviour

The function for the mass yield following fission is expected to be symmetric about half the mass of the fissioning nucleus in the liquid drop model. Observation of fission of the actinides totally disagrees with this expectation, and, as we have noted, is a major problem of the liquid drop model. Much lighter nuclides do exhibit symmetric fission however. Fig.18 illustrates the mass yield curves of the heavy fragments for some polonium isotopes[37]. These can be fitted well by a Gaussian function over most of the range, but there is an excess in the region of $A = 130$ to 145. These divisions are also associated with an anomaly in the total kinetic energy of the fragments, which is anomalously high (at low excitation energy of the fissioning nucleus) and has wide dispersion in its spread, as shown in the lower part of Fig.18 for ^{210}Po.

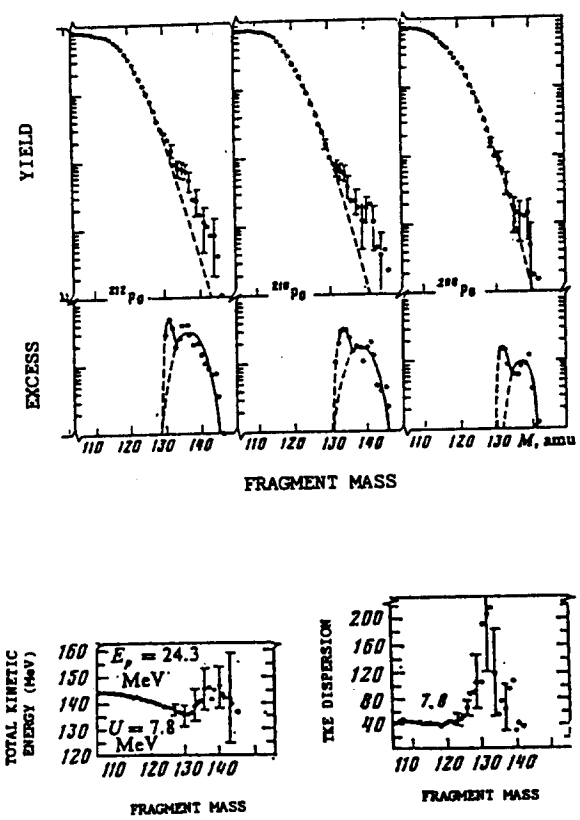

Figure 18. Top: mass yield functions for Po isotopes, and deviations from Gaussian. Below: total kinetic energy of fragments.

An explanation for such an effect can be sought in potential energy diagrams for the incipient fission products[38] as shown in Figs.19 and 20. These show energy contours as a function of deformation and proton or neutron number. The strong spherical shell effects at Z=50 and N=82 will give some lowering of the potential energy in the route towards division with a mass $\approx$ 132 fragment, as is apparent in Fig.21, which indicates "terraces" appearing at such mass divisions high above the symmetric valley floor as the neck radius of the fissioning nucleus diminishes[39]. They will also increase the total kinetic energy in the following way. The energy distribution at the scission point may be written

$$Q = TKE + TXE$$

where TKE is the total kinetic energy in the system at scission and TXE is the internal or "excitation" energy. These two terms can be further subdivided as

TKE = Coulomb repulsion energy of nascent fragments
+ pre-scission Kinetic Energy

and

TXE = Deformation energy of
nascent fragments
+ internal excitation energy

The pre-scission kinetic energy can be assumed to be negligible for fissioning compound nuclei with low excitation energy. Thus, if the deformation energy of the nascent fragments is low the Coulomb repulsion energy, which ultimately appears as the measured total kinetic energy, is higher than it would be in the liquid drop model.

But the spherical shell effects at A = 132 are not the only strong energy effects to be found. Reference to Fig.20 shows a strongly deformed neutron shell at N ≈ 88, which could well fortify the excess of mass 140 fission products seen in Fig.18.

With increasing mass and charge numbers of the fissioning nucleus asymmetric division becomes more likely. Very extreme forms of mass division are even found in the

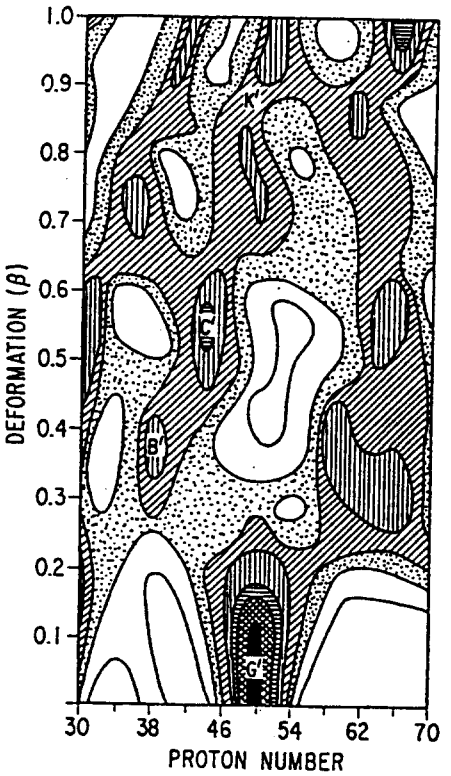

Figure 19. Shell energy corrections calculated for incipient fission products asfunction of Z and quadrupole deformation. Dark shading indicates low energy and light is high.

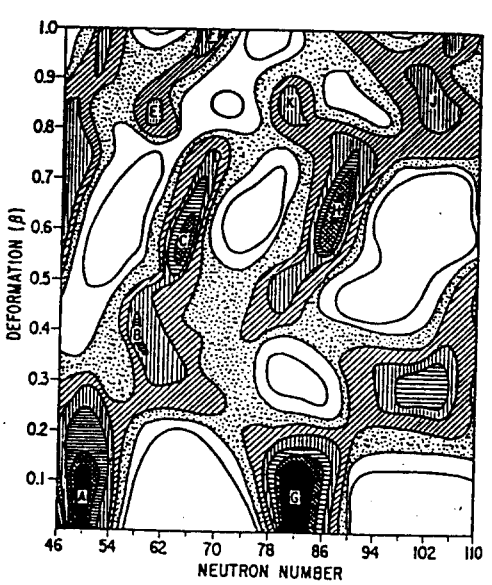

Figure 20. Shell correction energy in incipient fragments as function of neutron number and deformation.

phenomenon of "heavy-ion radioactivity"[40] (with emission of a range of fragments from ^{14}C to ^{28}Mg, depending on the mass of the radioactive nucleus[41]) that is explained theoretically as the shell closure effect in the Z = 82, N = 126 incipient fragment[42]. In the radium and actinium nuclei asymmetric fission centred about the A ≈ 140 heavy fragment peak is so strong that the triple mass peak yield curve discovered by Jensen and Fairhall[43] results; an example[44] is shown in Fig.22. Again the strongly asymmetric divisions are associated with higher than expected total kinetic energy. The triple peaks are evidence in themselves of two distinct modes of fission, possibly reached by two separate valleys through the energy surface from saddle to scission. An example of a calculated

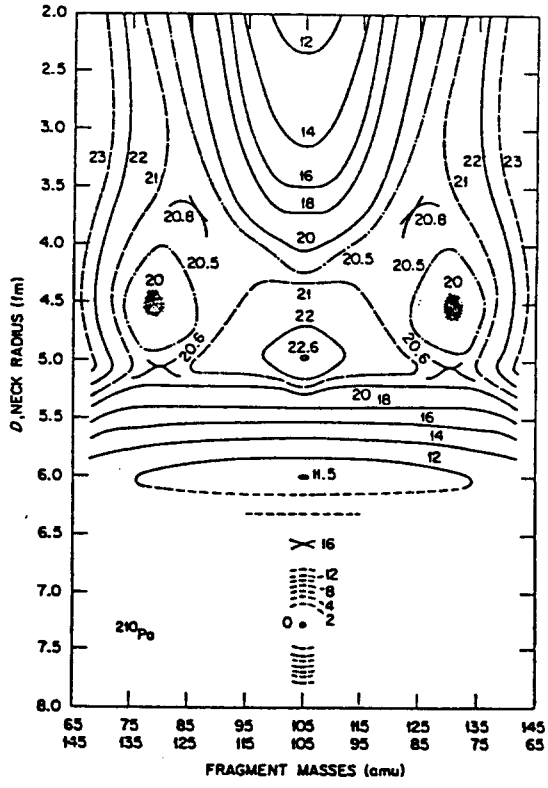

Figure 21. Potential energy diagram for ^{210}Po as function of neck radius (representing increasing elongation) and fragment mass (representing reflection asymmetry.

potential energy surface[45] (using Strutinsky theory) is shown for ^{228}Ra in Fig.23; it clearly demonstrates two separate cols leading to valleys with quite different mass asymmetry.

More strong evidence for the two mode hypothesis is provided by differential cross-section measurements for asymmetric and symmetric division[46]. In Fig.24 the cross-sections from the ^{226}Ra(^{3}He,d)^{227}Ac→f reaction show a more than 1 MeV difference in fission barrier for the two modes of mass division, and in Fig.25 a similar effect is shown for the fission of ^{228}Ra excited by the t,pf reaction[47].

Beyond radium, symmetric mass division becomes very weak for low energy fission. The double-humped mass yield curve that is characteristic of actinide fission has the feature that the heavy particle peak remains centred around mass 137 throughout the actinide range (as shown, for example[48], in Fig.27), the light particle peak rising in mass as the mass of the fissioning nuclide rises. This phenomenon clearly has the same explanation as for asymmetric fission throughout the polonium to radium region. The now strong influence of the Z = 50 and N = 82,88 shells dominates the valley from saddle to scission, as seen by the potential energy calculation[39] in Fig.26. Note from this diagram that it does not seem to be the entry point to the valleys at the saddle point that have the controlling influence on the ultimate mass division, but rather the mature valley configurations several MeV below.

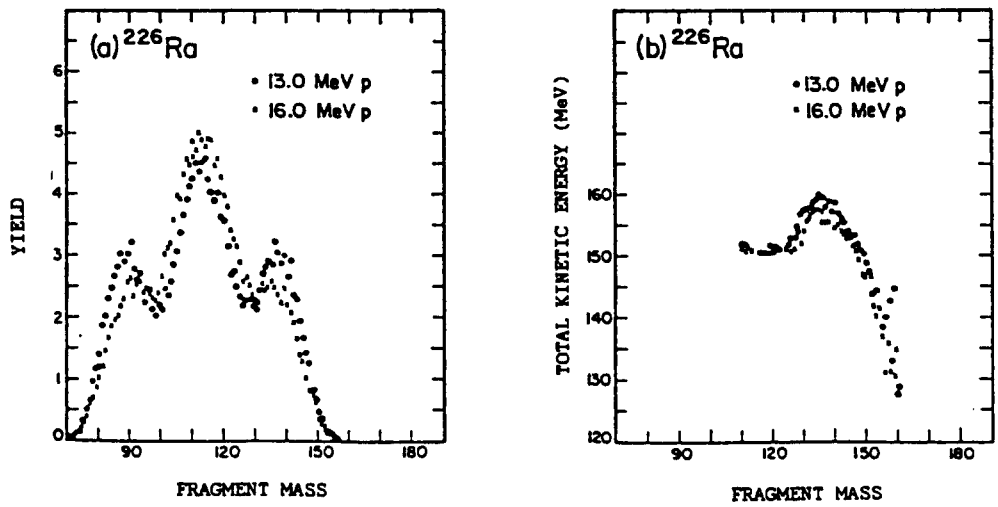

Figure 22. Mass yield and Total Kinetic Energy distributions for ^{226}Ra

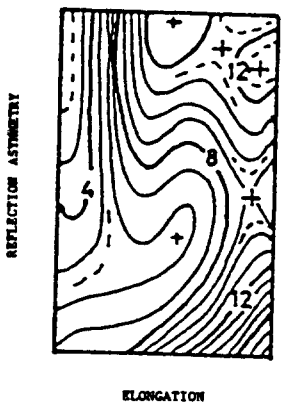

Figure 23. Potential energy surface for ^{226}Ra.

The validity of shell concepts near the scission point is also well illustrated by the recent precise experimental work at ILL on "cold fragmentation", in which events with high total kinetic energy are selected, thus leaving the incipient fragments with very little internal excitation energy at the scission point. Two of the mass yields of ^{234}U as measured on the fission product mass spectrometer Lohengrin for different total kinetic energies[49] are shown in Fig.28. The dominance not only of the heavy mass product A = 132, but also A = 144 (associated with the N = 88 deformed shell), is apparent. The probable mechanism for achieving such cold events has also been studied in terms of topographical features of the potential energy surface[50]. In Fig. 29 the surface as calculated by Hartree-Fock methods is shown as a function of both quadrupole and hexadecapole deformation variables; the cold events are achieved by tunneling in the hexadecapole direction through the ridge to give rapid necking at relatively small elongations.

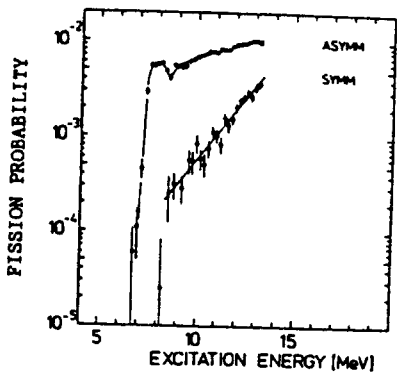

Figure 24. Fission probabilities for symmetric and asymmetric fission as function of excitation energy for ^{227}Ac.

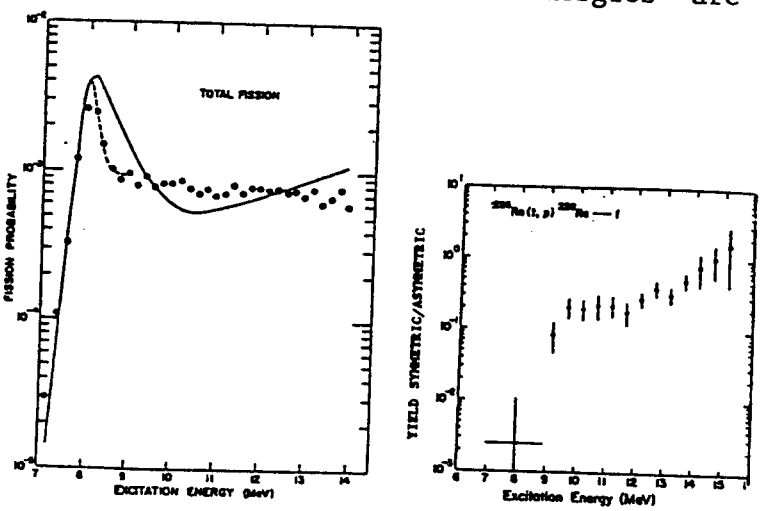

Figure 25. Total fission probability and ratio for symmetric and asymmetric fission of ^{226}Ra.

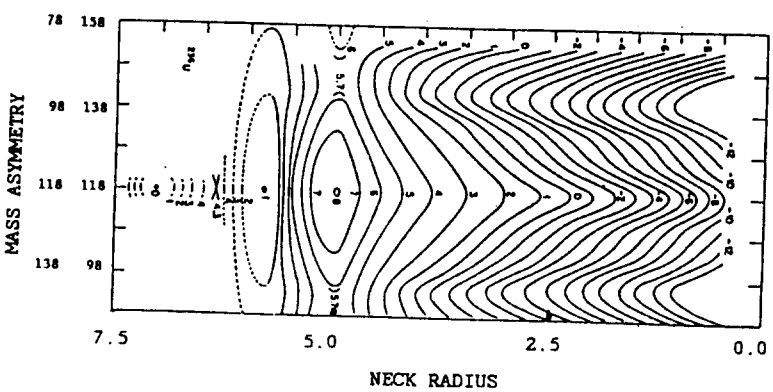

Figure 26. The calculated potential energy surface for ^{236}U.

The heaviest transuranics are marked by a sudden change in the fission product properties. Fig.30 shows mass yield curves for the californium isotopes[51], demonstrating the approach of the light and heavy peaks, but still with predominantly asymmetric division. Fig.31 shows the transition to the fermium[52] isotopes and illustrates both the mass yield and total kinetic energy behaviour. Clearly at ^{257}Fm there

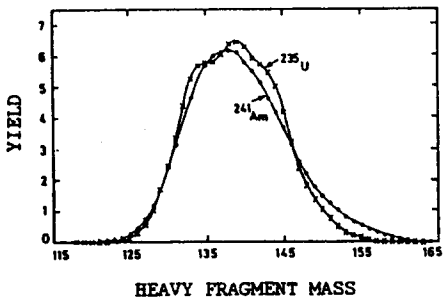

Figure 27. Heavy fragment mass yield function for slow neutron-induced fission of ^{235}U and ^{241}Am.

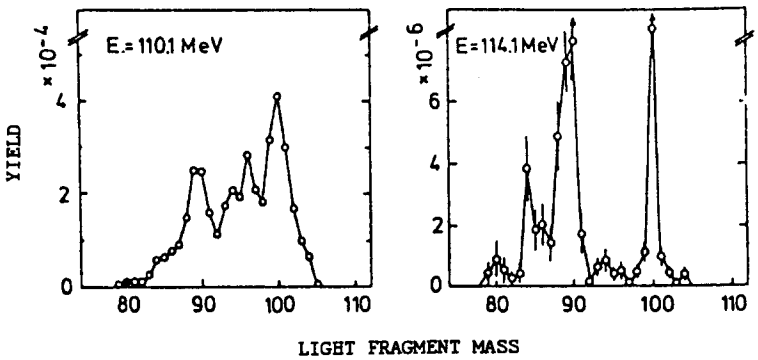

Figure 28. Light fragment yields at high kinetic energies for ^{234}U.

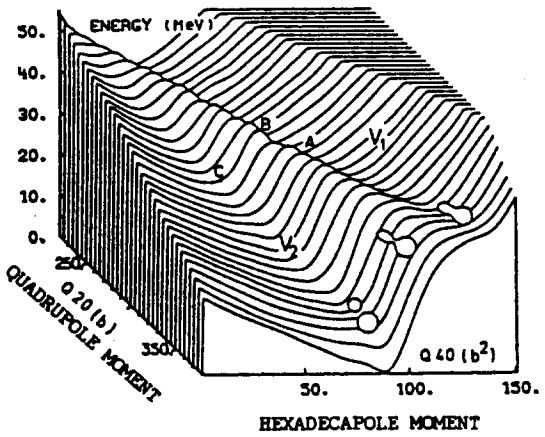

Figure 29. Potential energy surface of ^{240}Pu, near scission with respect to quadrupole and hexadecapole deformation

this being a spherical shell closure there is almost no deformation energy to go into excitation of separated fragments; hence total kinetic energy is high. The highly skewed distribution of kinetic energy shows that the shell favoured division is not the only mode of fission of these nuclides. That there are apparently two modes is shown in Fig.34 where the skewed form is analyzed convincingly into two gaussians with over 40 MeV difference in mean kinetic energy. Again, detailed potential energy calculations[33] indicate that there are two routes or saddle points across the barrier. An example for ^{258}Fm is shown in

is a sudden onset of symmetric events with very high total kinetic energy. This high total kinetic energy differentiates this kind of symmetric fission from that of the the much lighter fissioning nuclides in the polonium region. The heavier fermium isotopes show predominantly symmetric fission[33] (Fig.32) as do higher charge nuclides (Mendelevium, Nobelium, etc.) as shown in Fig.33, which also shows their total kinetic energy distribution[34].

The principal explanation of symmetric fission in these nuclides is the approach of the double shell closure Z = 50, N = 82 for both incipient fission products. With

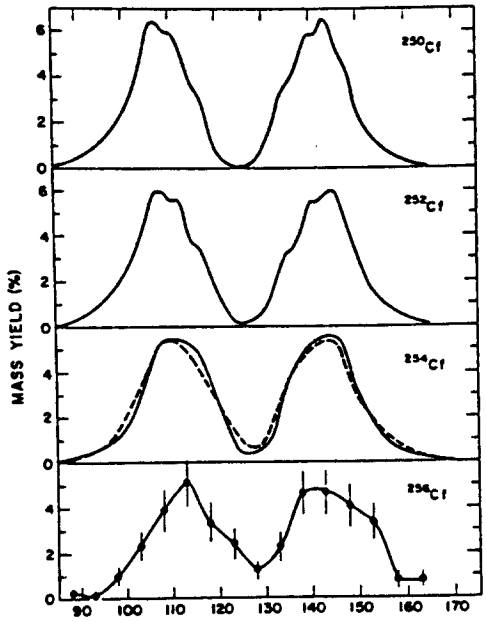

Figure 30. Mass yield distributions for californium isotopes.

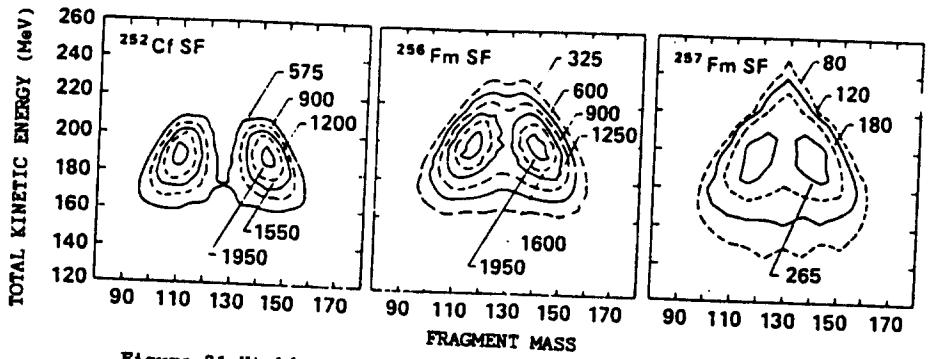

Figure 31. Yield contours as functions of total kinetic energy and mass for spontaneous fission of ^{252}Cf and $^{256,257}Fm$

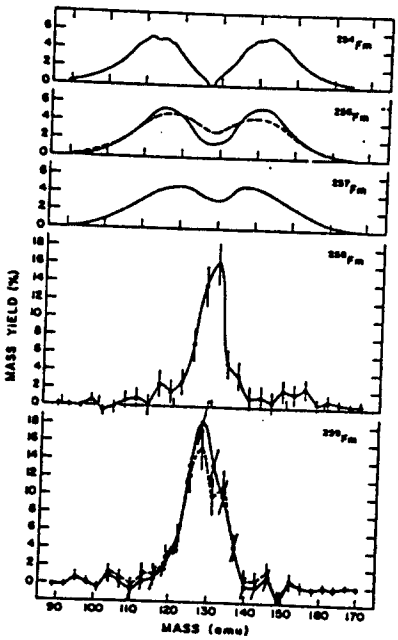

Figure 32. Mass yield curves for fermium isotopes.

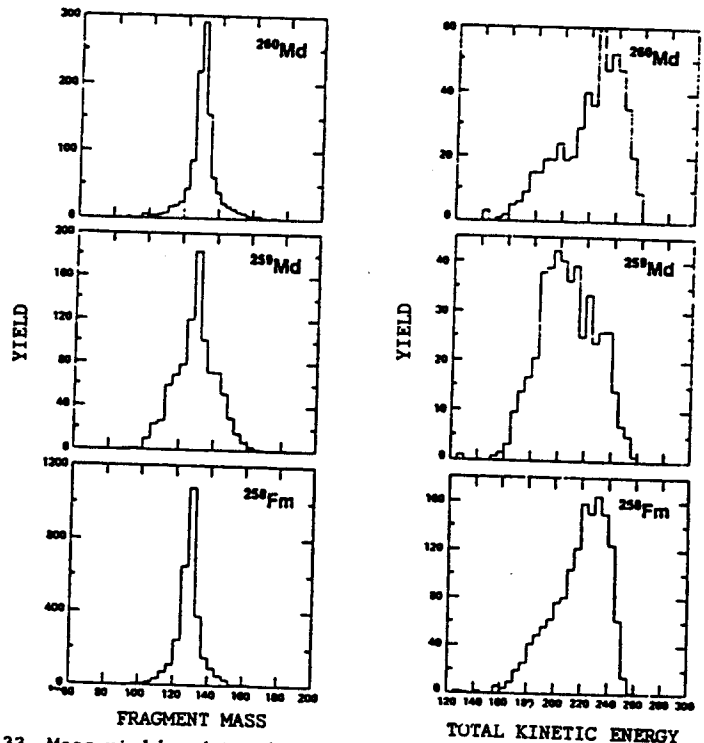

Figure 33. Mass yield and total kinetic energy histograms from spontaneous fission of trans-fermium nuclides near mass number 260.

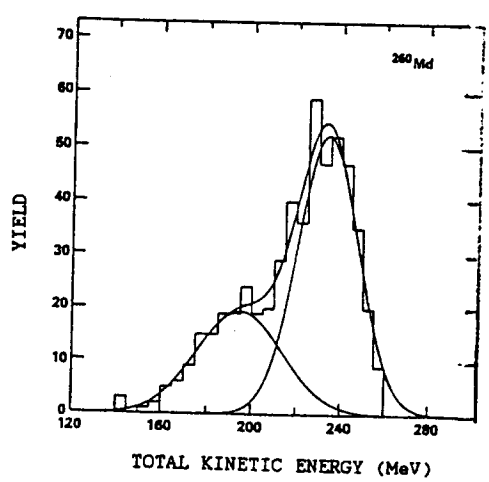

Figure 34. Analysis of Total kinetic energy distribution of ^{260}Md demonstrating the existence of two modes.

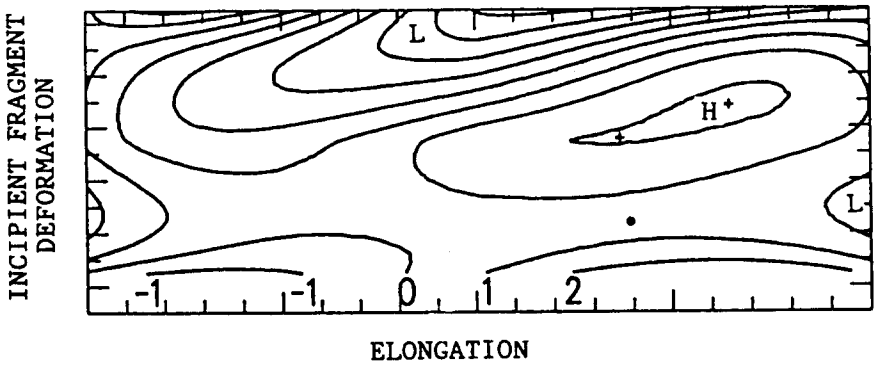

Figure 35. Potential energy contours in the cut through deformation space representing incipient fragment deformation and elongation for ^{256}Fm.

Fig.35. The potential energy contours are shown for the cut minimised against the mass reflection deformation variable, which in this case is close to symmetry. The abscissa represents elongation while the ordinate represents the total of incipient fragment deformation. There are apparently two saddle points in this diagram, one leading to low fragment deformation (and high kinetic energy) and the other to higher deformation and therefore to "hot" fragmentation. The former is presumably associated with the sharp component of the symmetric mass yield peak, and the latter with its broader underlying base.

8. Summary

In this short review of fifty years of nuclear fission I have attempted to illustrate the two main themes in the development of our understanding of the phenomenon. In the first 25 years, the subject was dominated by the concept of the electrically charged liquid drop that was the key to unlocking the initial dramatic discovery in 1939. Important modifications of the liquid drop concept emerged in that time, notably the introduction of the quantal modes of collective motion, but the influence of the major feature of nuclear structure theory, the importance of independent nucleon motion and the energy stabilization due to closed shells, did not appear until the end of that period. The second 25 year period has been dominated by the discovery of fission features and overall trends that can only be explained by the importance of nucleon shell effects in highly deformed nuclei. Most of the theory I have described here is semi-quantitative in the sense that only the potential energy surfaces as functions of deformation have been invoked. This is the static picture. The dynamic picture requires also the calculation of the inertial tensor through deformation space. Such theory is much more fragmentary at the present time. While independent particle motion and shell effects undoubtedly play a role here there seems to be much less confidence in the accuracy with which the inertial tensor can be calculated from first principles, and resort is still made to semi-empirical models. This will undoubtedly be the area in which the main effort and progress in the study of fission will be made in the coming years.

References

1. Fermi E 1934 *Nature* **133**,898
2. See E.Segre, *Ann.Rev.Nucl.Sci.***31**,(1981)
3. Noddack-Tacke I 1934 *Zeit.f.Ang.Chemie* **37**,653
4. Curie I and Savitch P 1938 *Comptes Rendues, Acad.Sci.Paris* **206**,1643
5. Hahn O and Strassmann F 1939 *Naturwissenschaften* **27**,11
6. Meitner L and Frisch O 1939 *Nature* **143**,239
7. Frisch O 1939 *Nature* **143**,276
8. Van Assche P H M 1988 *Nucl.Phys.***A480**,205
9. See S.R.Weart, *Physics Today*, Feb.1976,p.23
10. Anderson H L, Booth E T, Dunning J R, Fermi E, Glasoe G N and Slack F G 1939 *Phys.Rev.* **55**,511; McMillan E, *Phys.Rev.***55**,510; Roberts R B, Meyer R C and Hastad L R, *Phys.Rev.***55**,416
11. Anderson H L, Fermi E and Halstein H B 1939 *Phys.Rev.***55**,797; Anderson H L, Fermi E and Szilard L 1939 *Phys.Rev.***56**,284
12. Von Halban H, Joliot F and Kowarski L 1939 *Nature* **143**,470
13. Szilard L and Zinn W 1939 *Phys.Rev.***55**,799
14. Ladenburg R, Kanner M H, Barschall H H and Van Voorhis C C 1939 *Phys.Rev.***56**,168
15. Roberts R B, Meyer R C and Wang P 1939 *Phys.Rev.***55**,510
16. Booth E T, Dunning J R and Slack F G 1939 *Phys.Rev.***55**,981
17. Bohr N and Wheeler J A 1939 *Phys.Rev.***56**,426; see also E.Feenberg, *Phys.Rev.***55**,504 and J.Frenkel, *Phys.Rev.***55**,987
18. Bohr N 1939 *Phys.Rev.***55**,418
19. Fong P 1956 *Phys.Rev.* **102**, 434
20. Bohr A 1956 in *Proc. int.conf.on Peaceful Uses Atomic Energy, Geneva,1955 (United Nations, New York)* **2**,220
21. Hill D L and Wheeler J A 1953 *Phys.Rev.* **89**, 1102
22. Flerov G N and Polikanov S M 1964 *Compt.Rend.Cong.Int.Phys.Nucl.(Paris)* **1**, 407
23. Strutinsky V M 1967 *Ark.Fys* **36**, 629; *Nucl.Phys.* **A95**, 420
24. Migneco E and Theobald J P 1968 *Nucl.Phys.* **A112**, 603
25. Paya D, Blons J, Derrien H, Fubini A, Michaudon A and Ribon P 1968 *J.Phys.(Paris)* **29**, 159
26. Bjørnholm S, Borggreen J, Westgård L, Karnauchov V A 1967 *Nucl.Phys.***A95**,513
27. Britt H C, Burnett S C, Erkkila B H, Lynn J E and Stein W E 1971 *Phys.Rev.* **C4**,1444
28. Specht H J, Weber J, Konecny E and Heunemann D 1972 *Phys.Lett.* **41B**, 43
29. Kolar W. and Böckhoff K. 1968 *J.Nucl.En.* **22**, 299
30. Auchampaugh G F and Weston L W 1975 *Phys.Rev.* **C12**, 1850
31. Difillipo F C, Perez R B, de Saussure G, Olsen D K and Ingle R W 1977 *Nucl.Sci.Eng.***63**,153
32. Auchampaugh G F, de Saussure G, Olsen D K, Ingle R W, Perez R, Macklin R L 1986 *Phys.Rev.* **C33**, 125
33. James G D, Lynn J E and Earwaker 1972 *Nucl.Phys.* **A189**,225
34. Åberg S, Larsson S E, Möller P and Nilsson S G 1980 in *Physics and Chemistry of Fission* proc.conf.Jülich(IAEA,Vienna) **2**,299
35. Blons J, Mazur C, Paya D, Ribrag M and Weigmann H 1984 *Nucl.Phys.***A414**,1
36. Lynn J E 1983 *J.Phys.G* **9**,665
37. Itkis M G, Okolovich V N, Rusanov A Yu, Smirenkin G N 1984 *Sov.J.Nucl.Phys.* **39**, 852
38. Wilkins B D, Steinberg E P and Chasman R R 1976 *Phys.Rev.* **C14**,1832
39. Mustafa M G, Mosel U and Schmitt H W 1973 *Phys.Rev.* **C7**,1523

40. Rose H J and Jones G A 1984 *Nature* **307**, 245
41. Price P B 1988 in *proc.int.conf.on Nuclei far from Stability, Lake Rousseau* AIP conf.proc.**164**,800; Price P B, Stevenson J D, Barwick S W and Ravn H L 1985 *Phys.Rev.Lett.***54**,297
42. Sandalescu A, Poenaru D N and Greiner W 1980 *Sov.J.Nucl.Phys.* **11**, 528
43. Jensen R C and Fairhall A W 1958 *Phys.Rev.* **109**,942
44. Perry D G and Fairhall A W 1977 *Phys.Rev.* **C4**,977
45. Pauli H C 1973 *Phys.Rep.* **7**,35
46. Konecny E, Specht H J and Weber J 1973 *Phys.Lett.* **4B**,329
47. Weber J, Britt H C, Gavron A, Konecny E, Wilhelmy J B 1976 *Phys.Rev.***C13**,2413
48. Asghar M, Caïtucoli F, Perrin P, Barreau G, Guet C R, Leroux B and Signarbieux C 1979 in *Physics and Chemistry of Fission* proc.conf.Jülich (IAEA,Vienna) 2,81
49. Quade U, Rudolph K, Armbruster P, Clerc H, Lang W, Kutterer M, Pannicke J, Schmitt C, Theobald, J P, Gönnenwein F and Schrader 1982 *Lecture Notes in Physics* **158**, 40
50. Berger J-F, Girod M and Gogny D 1981 *J.Phys.Lettres* **42** L509
51. Hoffman D C 1979 in *Physics and Chemistry of Fission* proc.conf.Jülich (IAEA,Vienna) **2**,275
52. Balagna J P, Ford G P, Hoffman D C and Knight J D 1971 *Phys.Rev.Lett.* **26**,145
53. Hulet E K, Wild J F, Dougan R J, Lougheed R W, Landrum J H, Dougan A D, Schädel M, Hahn R L, Baisden P A, Henderson C M, Dupzyk R J, Sümmerer K, Bethune G 1986 *Phys.Rev.Lett.* **56**,313
54. Hulet E K 1988 in *proc.int.conf.on Nuclei far from Stability, Lake Rousseau* AIP conf.proc.**164**,810